An extended reservoir of class-D beta-lactamases in non-clinical bacterial strains

Valérian Lupo [1,2], Paola Sandra Mercuri [2], Jean-Marie Frère [2], Bernard Joris [2], Moreno Galleni [2], Denis Baurain [1,#], Frédéric Kerff [2,#]

[1] InBioS-PhytoSYSTEMS, Eukaryotic Phylogenomics, University of Liège, Liège, Belgium
[2] InBioS, Center for Protein Engineering, University of Liège, Liège, Belgium

Address correspondence to:
Denis Baurain: denis.baurain@uliege.be
Frédéric Kerff: fkerff@uliege.be

Keywords

antimicrobial resistance, beta-lactamase, phylogenetic classification, sequence clustering, carbapenemase, OXA

Abstract

Bacterial genes coding for antibiotic resistance represent a major issue in the fight against bacterial pathogens. Among those, genes encoding beta-lactamases target penicillin and related compounds such as carbapenems, which are critical for human health. Beta-lactamases are classified into classes A, B, C and D, based on their amino acid sequence. Class D enzymes are also known as OXA beta-lactamases, due to the ability of the first enzymes described in this class to hydrolyze oxacillin. While hundreds of class D beta-lactamases with different activity profiles have been

isolated from clinical strains, their nomenclature remains very uninformative. In this work, we have carried out a comprehensive survey of a reference database of 80,490 genomes and identified 24,916 OXA-domain containing proteins. These were deduplicated and their representative sequences clustered into 45 non-singleton groups derived from a phylogenetic tree of 1413 OXA-domain sequences, including five clusters that include the C-terminal domain of the BlaR membrane receptors. Interestingly, 801 known class D beta-lactamases fell into only 18 clusters. To probe the unknown diversity of the class, we selected ten protein sequences in ten uncharacterized clusters and studied the activity profile of the corresponding enzymes. A beta-lactamase activity could be detected for seven of them. Three enzymes were active against oxacillin and two against imipenem. These results indicate that, as already reported, environmental bacteria constitute a large reservoir of resistance genes that can be transferred to clinical strains, whether through plasmid exchange or hitchhiking with the help of transposase genes.

Importance

The transmission of genes coding for resistance factors from environmental to nosocomial strains is a major component in the development of bacterial resistance towards antibiotics. Our survey of class D beta-lactamase genes in genomic databases highlighted the high sequence diversity of the enzymes that are able to recognize and/or hydrolyze beta-lactam antibiotics. Among those, we could also identify new beta-lactamases that are able to hydrolyze carbapenems, one of the last resort antibiotic families used in human chemotherapy. Therefore, it can be expected that the use of this antibiotic family will fuel the emergence of new beta-lactamases into clinically relevant strains.

Introduction

Beta-lactamases are the main enzymes responsible for the resistance of bacteria to beta-lactams, which are the major antibiotics utilized in the fight against pathogenic bacteria. Even before the structure of penicillin was known, Abraham and Chain (1) described “An enzyme from bacteria able to destroy penicillin” and, in the late 40’s and early 50’s, the staphylococcal beta-lactamase became an important source of clinical problems solved by the introduction of methicillin (2, 3). Later, an ever increasing number of these hydrolases have been identified. These can be classified into four classes based on their primary structures. Classes A, C and D are active-serine enzymes (4) while class B consists of metallo-proteins whose active site usually contains 1 or 2 Zn^{++} ions (5, 6).

Beta-lactamases of classes A and D exhibit a very high diversity of amino acid (AA) sequences, with only a very little number of conserved residues within each class (e.g., 29 residues are conserved within class-A beta-lactamases) (7). It is nearly impossible to establish clear relationships between AA sequences and the ability to hydrolyse specific classes of beta-lactam antibiotics. Indeed, it is well known that a single mutation can alter this activity profile in a significant manner (8, 9). Moreover, the literature contains numerous disagreements and errors concerning the kinetic parameters of various enzymes (10). This is probably in part because these parameters are often determined under different experimental conditions and the studied enzymes are not always pure. In consequence, even though clinicians are more interested in specificity profiles, the AA sequences remain the primary tool for proposing a classification of beta-lactamases, as in the case of the Beta-Lactamase

3

Database (BLDB; http://www.bldb.eu/) (11). Concerning class D beta-lactamases, the situation is complicated by the fact that these enzymes can dimerize, which sometimes modifies the activity (12) and that carboxylation of the first conserved motif lysine also increases the activity in most cases (13). Inversely, loss of CO_2 during turn-over of the substrate results in “substrate-induced inactivation”, a phenomenon already observed by Ledent et al (14).

The first two identified class D beta-lactamases exhibited a number of features that differed from those of nearly all beta-lactamases known at the time, notably the ability to efficiently hydrolyze oxacillin and other isoxazolyl penicillins. For this reason, they were named OXA-1 and OXA-2. Unfortunately, it was then decided to name the further class D beta-lactamases homologs “OXA” plus sequence (i.e., increasing) number that follows the chronological order of identification (15). This was sometimes done in spite of a sequence identity below 30% and/or (10) more similarity with the BlaR receptor than with other class D beta-lactamases (16). Class D beta-lactamases were first identified as plasmid-encoded proteins but the corresponding genes were later found to reside on the bacterial chromosome too (10).

Similarity searches using the OXA-2 AA sequence as query revealed homologous primary structures of unknown function or without true beta-lactamase activity, such as YbxI/BSD-1 in *Bacillus subtilis* (17, 18), or even devoid of any beta-lactamase activity, such as the C-terminal domain (CTD) of the BlaR penicillin-receptor involved in the induction of a class A beta-lactamase in *Bacillus licheniformis* and *Staphylococcus aureus* (19). In the present study, proteins containing a class-D

beta-lactamase domain will be further referred to as the “OXA-domain family”. Among those, “DBL” will be reserved to demonstrably active class-D beta-lactamases, while characterized class-D beta-lactamase homologs of low activity or with a different function will be termed “pseudo-DBL” proteins. Finally, “DBL-homolog” proteins will design the union of DBL, pseudo-DBL proteins, and other homologs not yet characterized.

It is clear that our present knowledge of the OXA-domain family is biased toward clinically relevant DBLs. The analysis of whole genome sequences of isolated bacteria and metagenome-assembled genomes highlighted that non-pathogenic and environmental bacteria can also harbor beta-lactamase-encoding genes, and thus may behave as reservoirs of emerging new resistant genes identified in nosocomial strains (20, 21). It is likely that these bacteria, which were never exposed to synthetic or semi-synthetic beta-lactams used in human health care or animal husbandry, can encounter other beta-lactam-producing microorganisms in their natural environment and, over the ages, have acquired beta-lactamase genes in their “struggle for life” (22). A significant example could be the carbapenems that can be produced by some *Streptomyces* species (23), probably resulting in the appearance of the carbapenemases that were later transferred to clinical strains (24, 25). The large heterogeneity of the resistance gene repertoire present in bacteria challenges the efficiency of chemotherapy. It also underlines the need to develop new analytical methods allowing a clear and rapid identification of potential new resistance pathways including enzymes that can inactivate both old and new antibiotics.

The goals of the present article were to explore genomic databases to discover how

widespread the class D beta-lactamase gene and its homologs were throughout the microbial world and to propose a sequence-based classification of the members of the OXA-domain family derived from their phylogenetic relationships. Starting from 80,490 genomes, we identified a total of 24,916 DBLs and DBL-homolog sequences, which we classified into 64 clusters of proteins. Furthermore, we synthesized and expressed ten gene sequences sampled from ten clusters devoid of characterized members and conducted a survey of their activity. This revealed that three of them had an oxacillinase activity, including two able to hydrolase imipenem, reminding us how environmental bacteria represent an enormous reservoir of resistance factors that can be transferred to clinical strains.

Materials and Methods

SQL database

Bioinformatic data generated in this study was stored into a sqlite3 database (Figure S1). This database was exploited using SQL queries in order to generate additional results and statistics.

Reference class D beta-lactamase sequences and identification of OXA-domain family proteins

A total of 1617 unique beta-lactamases amino-acid sequences were downloaded from the NCBI Pathogen Detection server (ftp://ftp.ncbi.nlm.nih.gov/pathogen/) on the 1st of December 2017. Among those, 470 DBL were retrieved based on metadata and accession numbers. DBL protein sequences were deduplicated using

CD-HIT v4.6 (26) with a global sequence identity threshold of 0.98 and then aligned using MAFFT v7.273 (27). An HMM profile was constructed from the DBL alignment using the HMMER package v3.1b2 (28) to identify OXA-domain family proteins in a local prokaryotic protein sequence database. This local database was built on 7th of December 2017 using the protein sequences of 80,490 prokaryotic genome assemblies stored in the NCBI RefSeq database. OXA-domain family proteins were graphically selected using the ompa-pa.pl interactive software package (A. Bertrand and D. Baurain; https://metacpan.org/dist/Bio-MUST-Apps-OmpaPa) and taxonomically annotated using the NCBI Taxonomy.

Annotation of OXA-domain family proteins

OXA-domain family proteins were tagged using a BLAST-based annotation script (part of Bio-MUST-Drivers) with an identity threshold from 90% to 100% and an e-value threshold of 1e-20. DBL-homolog sequences used for the annotation were downloaded from the BLDB (http://www.bldb.eu/BLDB.php?prot=D) (11) on the 22nd of July 2019, to which were added three sequences of the membrane receptor BlaR from *Clostridium difficile* (CDT53463.1), *Staphylococcus aureus* (P18357) and *Bacillus licheniformis* (P12287), the bifunctional class C/class D beta-lactamase LRA13-1 (ACH58991.1) (20) and the two intrinsic pseudo-DBLs of *Clostridium difficile* CDD-1 (CZR76508.1) and CDD-2 (SJQ22628.1) (29).

Domain characterization of OXA-domain family proteins

The potential presence of a signal peptide was predicted using local SignalP-5.0b (30). The organism option was set to ‘gram+’ for sequences belonging to Firmicutes and Actinobacteria and ‘gram-’ for the other phyla. To improve the prediction of

transmembrane helices with local TMHMM v2.0 (31), the signal peptide (if any) was first removed from the original sequences when the cleavage site prediction probability was greater or equal to 0.6. For sequences of intermediary length (i.e. between 350 and 550 AAs) and some long sequences (i.e. greater than 550 AAs), InterProScan v5.37-76.0 with default parameters and disabled use of the precalculated match lookup (32), along with pepwindowall with default parameters from the EMBOSS web portal (33) were used to distinguish between transmembrane segments and other extensions.

Localization and genetic environment of OXA-domain family proteins

A genetic environment database was built from the bacterial genomes featuring at least one OXA-domain family sequence using GeneSpy “3 in 1” module, as described in the manual (34). Contig accessions were retrieved from the database and the corresponding FASTA files were downloaded using the command-line version of the “efetch” tool from the NCBI Entrez Programming Utilities (E-utilities). PlasFlow v1.1 was used to predict potential plasmid sequences in the contig FASTA files (35).

Clinical strain determination

BioSample reports associated with bacterial organisms were also downloaded using efetch (see above). All words of a report were collected and fed to a script that renamed and standardized them using an OBO (Open Biomedical Ontologies) dictionary. A score was attributed to each standardized word: +1 for a “clinical” word, 0 for an uninformative word and -1 for a non-clinical word. At last, a final score was

computed for each BioSample according to its collection of standardized words (see figshare). A bacterial strain was considered as “clinical” when its metadata was associated with a positive score, “non-clinical” for a negative score and not classified for a null score.

Alignment and phylogenetic analysis

After deduplication using CD-HIT v4.6 (26) with a global sequence identity threshold of 0.95, OXA-domain family protein sequences were aligned using MAFFT v7.273 (27). Alignments were then carefully optimized by hand using the program “ed” and alignment columns were manually selected using the program “net”, both part of the MUST software package (36). The resulting matrix of 1413 sequences x 188 unambiguously aligned AAs was used to infer a phylogenetic tree with RAxML v8.1.17 (37) under the LG+F+G4 model. Support values were initially estimated through 100 fast bootstrap pseudo-replicates with RAxML then transformed into transfer bootstrap expectation (TBE) values using the booster algorithm (38).

Phylogenetic clustering

To produce clusters of related OXA-domain family sequences, the phylogenetic tree was first converted to a phylo4 object using the readNewick function of the phylobase R package (39). Then, a patristic distance matrix (dist.mat) was computed using the distTip function from the adephylo R package (40) and an adjacency matrix (adj.mat) was computed as follow:

$adj.mat = \frac{dist.mat}{\lim.p} < 1$ with $\lim.p = max(dist.mat) \times x$ and x varying from 0.10 to 0.50.

Clustering was performed by passing the adjacency matrix to the mcl function of the

9

MCL R package (41) with the addLoops option set to FALSE, allow1 set to TRUE and the inflation parameter varying from 1.0 to 3.0 by increments of 0.5. The best parameter combination was chosen by maximizing a score composed of the normalized entropy and the fraction of monophyletic clusters, following the method of Califice et al., 2012 (42). However, combinations yielding less than 15 clusters were discarded, regardless of their score, in order to avoid the grouping of most OXA-domain family sequences into a single cluster and retain the potential to provide a meaningful classification.

DBL-homolog genes selection for lab validation

Based on the phylogenetic clustering of OXA-domain family proteins, ten representative protein sequences (hereafter referred to as OXAVL01 to OXAVL10) spread among different clusters corresponding to DBL-homologs were selected as probes for the functional diversity. The criteria of selection were: (1) the sequence must belong to a cluster with more than five DBL-homologs and no DBL found in the BLDB, (2) the length of the sequence must lie between 250 and 350 AAs and the sequence must have no mutation in the three conserved motifs defining the class D active site (SxxK, SxV, KT/SG) (except if a mutation is shared by all the sequences of the cluster), (3) the sequence must be present in a bacterial species where no DBL is described according to the BLDB.

Gene synthesis and expression plasmids

Signal peptides of the ten selected sequences were removed and replaced by the PelB leader sequence (43). Then, the corresponding genes were synthesized after codon optimization for expression in *E. coli*. Expression plasmids of OXAVL01 to

10

OXAVL10 were purchased from Twist Bioscience (San Francisco, CA, USA). Briefly, the synthesized genes were cloned into pET 24a(+) (Novagen-Merck KGaA, Darmstadt, DE) and inserted between *Bam*HI (at the 5' end of the gene) and *Xho*I (at 3' end of the gene) restriction sites. All the enzymes were produced by *E. coli* BL21 (DE3) (Fisher Scientific SAS Illkirch Cedex, FR) carrying pOXAVL01-pOXAVL10 plasmids in LB medium supplemented with kanamycin 50 µg/mL (LB-kanamycin).

Antibiotics

Kanamycin was purchased from MP Biomedicals, cefotaxime, cephaloridine and oxacillin from Sigma Aldrich, cefazolin from Pharmacia & Upjohn SpA, imipenem from MSD, meropenem from Fresenius Kabi NV/SA, ampicillin from Fisher Scientific, amoxicillin from PanPharma, carbenicillin from Pfizer Italy, piperacillin from Lederle/AHP Pharma, temocillin from Eumedica N.V/S.A and nitrocefin from Abcam.

Assessment of soluble enzymes expression levels

Single colonies of *E. coli* BL21 (DE3) carrying the plasmids pOXAVL01 to pOXAVL10 were inoculated in 6 mL of LB medium supplemented with kanamycin. The precultures were incubated overnight (O/N) at 37°C with orbital shaking at 250 rpm. 2.5 mL of the different precultures were added to 100 mL of fresh LB-kanamycin. The bacteria were grown to an A_{600} of 0.7 and IPTG was added at a final concentration of 0.5 mM. The different cultures were divided in two, one incubated at 37°C and the other one at 18°C. Aliquots (1 mL) of the different cultures at 37°C were taken 0, 2, 4 hours after induction. In the case of the cultures incubated at 18°C, two aliquots (0 and 24 hours after induction) were analyzed. The different aliquots were centrifuged at 5,000 *g* for 10 min, the bacterial pellets were

resuspended in 25 mM HEPES buffer (pH 7.0) and sonicated (three times for 30 s each time at 12 W). Cell debris were eliminated by centrifugation at 13,000 *g* for 30 min. 20 μL of the soluble fractions and pellets were loaded onto a sodium dodecyl sulfate polyacrylamide gel (SDS-PAGE) (4-20%). The run was performed at a constant voltage (120 V). The beta-lactamase activity of the different fractions was determined by measuring the initial rate of hydrolysis of 100 µM Nitrocefin, 1 mM oxacillin, 1 mM ampicillin and 100 µM imipenem.

Production and purification of OXAVL02/06

A single colony of *E. coli* BL21 (DE3) pOXAVL02 or *E. coli* BL21 (DE3) pOXAVL06 was inoculated into 100 mL of LB-kanamycin. The preculture was incubated O/N at 37°C under agitation. 40 mL of the preculture was added to 1 liter of fresh LB-kanamycin. IPTG (100 µM final concentration) was added when the culture reached an A_{600} of 0.7. The cultures were incubated O/N at 18°C. Cells were harvested by centrifugation at 5,000 g for 10 min at 4°C. The pellets were resuspended in 15 mL 50 mM Sodium Phosphate, 0.5 M NaCl, 20 mM Imidazole pH 8.0 (buffer A) for pOXAVL02 and in 25 mM HEPES pH 7.0 (buffer B) for pOXAVL06. The bacteria were disrupted with a cell disrupter (Emulsiflex C3 Avestin GmbH, DE), which allows cell lysis at a pressure of 5,500 kPa. The lysates were isolated by centrifugation at 45,000 g for 30 min. The two supernatants were dialyzed O/N at 4°C against buffers A and B, respectively. The dialysed samples were then filtered through a 0.45 µm filter.

For OXAVL02, the supernatant was loaded onto Ni Sepharose® (24 mL) (GE Healthcare Europe GmbH, Freiburg, DE) previously equilibrated with buffer A. The enzymes were eluted with a gradient using 50 mM Sodium Phosphate pH 8.0, 0.5 M

12

NaCl, 0.5 M imidazole (buffer C). The fractions displaying a beta-lactamase activity were pooled, and then dialyzed O/N against buffer B and loaded onto a Source 15 Q column 20 mL (Pharmacia Biotech/ BioSurplus Inc., San Diego, CA, USA) equilibrated with the same buffer. The enzyme was eluted with a salt gradient using buffer B with 1 M NaCl, (buffer D). The fractions were pooled and loaded on a molecular sieve Superdex 75 GL 500 mL column (GE Healthcare Europe GmbH, Freiburg, DE) equilibrated in buffer B.

For OXAVL06, the cleared supernatant was loaded onto a 10 ml Q Sepharose® HP column (GE Healthcare Europe GmbH, Freiburg, DE) equilibrated in buffer B. The enzyme was eluted with a salt gradient using buffer D. The fractions with a beta-lactamase activity were pooled, and dialyzed O/N in 50 mM Sodium Phosphate pH 7.5, 0.5 M NaCl, 20 mM imidazole (buffer E). The dialysed sample was loaded onto Ni Sepharose® (24 ml) (GE Healthcare Europe GmbH, Freiburg, DE) previously equilibrated with buffer E. The enzymes were eluted with a gradient using 50 mM Sodium Phosphate pH 7.5, 0.5M NaCl, 0.5 M imidazole pH 7.5 . The active fractions were collected and concentrated by ultrafiltration on a YM-10 membrane (Amicon) to a final volume of 2 mL, then loaded onto a molecular sieve Superdex 75 GL (10/300) column (GE Healthcare Europe GmbH, Freiburg, DE) equilibrated in buffer B.

Conformational characterization of OXAVL02/06 by SEC-MALS

The oligomeric states of the DBL-homolog enzymes were analyzed by SEC-MALS (Treos II, WYATT Technology France, Toulouse Cedex 3, FR) (44). The experiments were performed using a HPLC Bio-inert Shimadzu Prominence LC-20Ai (SHIMADZU Benelux B.V) coupled to a SPD-20A UV/VIS detector and a RID-20 refractive index detector. The different active fractions isolated by size-exclusion chromatography

were dialyzed against a "SECMALS-PBS buffer" (Na_2HPO_4 10 mM, KH_2PO_4 1.8 mM, NaCl 137 mM, KCl 2.7 mM pH 7.4). Samples (100 µL OXAVL02 or OXAVL06 at 0.5-1 mg/mL) were loaded onto a Superdex® 200 Increase 10/300 G column (GE Healthcare Bio-Sciences AB Uppsala, SW) pre-equilibrated with the "SECMALS-PBS buffer". The column was calibrated by using Bovine Serum Albumin (BSA) (MM = 66,430 Da) as reference standard. The data acquisition of molecular mass, distribution of Monomer-Dimer equilibrium and percentage of aggregates were estimated using the ASTRA software (44).

Kinetic parameters determination

Steady-state kinetic parameters (K_m and k_{cat}) were determined by measuring substrate hydrolysis under initial rate conditions and using the Hanes–Woolf linearization of the Michaelis–Menten equation (45). Kinetic experiments were performed by following the hydrolysis of each substrate at 30°C in 50 mM HEPES buffer pH 7.5, 50 mM Na_2CO_3. The reactions were performed in a total volume of 500 µL at 30°C. BSA (20 µg/mL) was added to diluted solutions of beta-lactamase in order to prevent enzyme denaturation. The data were collected with a Specord 50 PLUS spectrophotometer (Analytik Jena, DE). Each kinetic value is the mean of three different measurements; SDs (standard deviations) were below 5%.

Data Availability

Publicly available datasets analyzed in this study can be found here: https://doi.org/10.6084/m9.figshare.18544955.

14

Results

Enlarging the OXA-domain family taxonomic distribution

According to the BLDB (as of July 2019), the 810 described DBL-homologs (including both DBL and pseudo-DBL proteins) have been isolated from bacteria belonging to five different phyla: Proteobacteria (583 sequences), Spirochaetes (14), Firmicutes (9), Bacteroidetes (1), Fusobacteria (1) and also from some marine metagenomes (2). 200 sequences have no source organism and are all plasmid-encoded. Most of these DBL-homologs are found in Proteobacteria, essentially in the genera *Acinetobacter* (411 sequences) and *Campylobacter* (91), which are part of the Gammaproteobacteria and Epsilonproteobacteria, respectively. Some are also found in Betaproteobacteria (41) but not in the other Proteobacteria classes.

A HMM profile constructed from an alignment of 470 DBL from NCBI Pathogen Detection server allowed us to identify 24,916 OXA-domain family AA sequences distributed across 20,342 organisms (on a total of 80,490 screened genome assemblies found in NCBI RefSeq). Nearly all those organisms (99.4%) belonged to the aforementioned five phyla, whereas the small remaining fraction (0.6%) came from eight additional bacterial phyla: Cyanobacteria (65 sequences), Actinobacteria (36), Chlorobi (10), Chlamydiae (6), Verrucomicrobia (6), Chloroflexi (2), Balneolaeota (1) and Planctomycetes (1). Moreover, some sequences were identified in additional classes of Proteobacteria: Alphaproteobacteria (Holosporales) and Deltaproteobacteria (Desulfovibrionales). In contrast, no sequences of the OXA-domain family were found in Archaea. In this work, we wanted to characterize the

15

353 protein sequences themselves and, to do so, we deduplicated the 24,916 sequences
354 and observed that they represented only 3510 unique sequences (i.e. 100% identical
355 at the AA level), indicating that many of them were multispecies enzymes. Indeed, it
356 is known that the NCBI RefSeq database is unevenly biased toward clinical strains
357 (46). Hence, 3459 of the unique sequences (98.5%) were found in several species of
358 the same genus (e.g. WP_001046004.1 was found in 952 *Acinetobacter* species)
359 while 51 unique sequences (1.5%) were found in more than one genus. These
360 results show that the redundancy is mostly due to the number of species in NCBI
361 RefSeq belonging to the same genus. In a second step, these 3510 unique
362 sequences were deduplicated at a global identity level of 95%, and the 1413
363 resulting sequences (hereafter termed 'representative' sequences) were used to
364 infer a phylogenetic tree (see Materials and Methods).

365 OXA-domain family proteins include BlaR homologs

366 A distribution of sequence length showed that the 24,916 OXA-domain family
367 sequences formed three populations, one shorter than 350 AAs with an average size
368 of 271 AAs (typical DBL length), one longer than 550 AAs with an average size of
369 587 AAs (typical BlaR membrane receptor length) and one intermediate-length
370 population with an average size of 449 AAs (Fig. 1a). Mapping sequence length onto
371 the tree revealed that representative sequences of intermediate length are scarce (5
372 sequences) and not clustered, whereas long sequences do cluster in two distinct
373 groups (Fig. 1b). A sequence similarity analysis showed that three of the five
374 intermediate-length sequences are actually DBL-homologs while two are BlaR
375 homologs. Regarding the two groups of long sequences, the larger one is formed of
376 sequences found in Firmicutes, with a majority in *Staphylococcus*, *Clostridioides* and

Bacillus. According to the annotation results, these sequences are actually BlaR homologs. The second group contains sequences found in Oxalobacteraceae (Betaproteobacteria) and annotation results at first showed no close similarity with DBL nor BlaR. However, detailed *in silico* functional analysis (InterProScan and pepwindowall; Supplemental Data 1) eventually revealed that 14 of these representative sequences indeed have a class D active site and the BlaR1 peptidase M56 domain, whereas three have both a class D active site and a class C beta-lactamase active site, like in the LRA-13 fusion enzyme (20), but these exhibit a low sequence identity to the latter (around 60%). To facilitate subsequent discussion, the three intermediate-length DBL homologues and the 3 OXA-class C fusion proteins were considered as DBL-homologs, whereas the two intermediate-length sequences more similar to BlaR and the two groups of long sequences were considered as BlaR-homologs.

In Firmicutes, beside the 10,496 BlaR-homologs, we also found 1383 DBL-homologs. According to the annotation results, 374 are homologous to low-activity pseudo-DBL proteins found in *Bacillus* (17, 18) and 956 are homologous to the two intrinsic pseudo-DBL (CDD) of *Clostridium difficile* (*Clostridioides difficile*) (29).

In general, surveyed bacteria possess only either one DBL-homolog protein (9964 strains) or one BlaR-homolog protein (5874 strains). In 1665 and 1813 strains, we found two DBL-homologs or two BlaR-homologs, respectively, and rarely more than two DBL-homologs (49) or BlaR-homologs (5). In addition, 963 strains simultaneously possess one DBL-homolog and one BlaR-homolog, while 10 strains show more than one DBL-homolog and one BlaR-homolog or the opposite (Fig. 1c).

Interestingly, strains that harbor more than one DBL-homolog (ignoring BlaR homologs) mostly belong to Pseudomonadales, and more specifically the genera *Acinetobacter* and *Pseudomonas*.

Gene genetic context

Among the 24,916 DBL-homolog and BlaR-homolog protein sequences initially identified, only 23,833 corresponding genes (found on 23,093 contigs) could actually be fetched from complete genomes. Three reasons explain the 1083 missing sequences: (1) the genome has been suppressed during the study, (2) the sequence has been suppressed or removed at the submitter's request and could not be found in the genome annotation (gff) file, (3) no link between the protein and any gene exists in the NCBI. According to the NCBI annotation pipeline, the contigs are classified "chromosome" in 960 cases, "plasmid" in 273 cases and "genomic" in 21,860 cases. This rather uninformative "genomic" classification led us to predict the genetic context of each OXA-domain family protein sequence using the dedicated PlasFlow pipeline. With this strategy, 15,515 contigs were classified as "chromosome" (67.2%), 5660 as "plasmid" (24.5%), whereas 1918 remained unclassified. These unclassified contigs correspond to 9.20% of the DBL-homolog genes (1327 cases) and 5.79% of the BlaR-homolog genes (608 cases). 1177 contigs were congruently classified (either as chromosome or plasmid) by both pipelines, and only four had different labels, thereby confirming the accuracy of PlasFlow for contig classification. DBL-homolog and BlaR-homolog genes are mostly chromosome-encoded (Fig. 2a), with 10,078 (69.89% of DBL-homolog genes) and 6153 (58.62% of BlaR-homolog genes) cases, respectively, whereas the genes are plasmid-encoded in 2159 and 3508 cases, respectively. Thus, 14.97% of DBL-

426 homolog genes and 33.42% of BlaR-homolog genes lie on a plasmid.

427

428 The majority of bacteria carrying an DBL-homolog gene on a plasmid belong to six
429 genera of Gammaproteobacteria: *Acinetobacter* (724), *Klebsiella* (590), *Escherichia*
430 (212), *Shigella* (200), *Enterobacter* (196) and *Pseudomonas* (85). The remaining
431 plasmid-encoded sequences are distributed across the other classes of
432 Proteobacteria (Alpha- (35), Beta- (46) and Gammaproteobacteria (61)), while a few
433 can also be found in Firmicutes (6), Cyanobacteria (3) and Bacteroidetes (1).

434

435 To assess the transfer potential of DBL-homolog and BlaR-homolog genes, and
436 therefore the propensity of emergence of a new resistance, we looked for
437 transposase genes in the vicinity of these genes (Fig. 2b). We noticed that DBL-
438 homolog and BlaR-homolog genes are either close to transposase genes (distance
439 from one to five genes) or very distant (more than 15 genes) in each genetic context.
440 Concerning BlaR-homologs, 63.4% of the genes are close to at least one
441 transposase gene when chromosome-encoded and 67% when plasmid-encoded.
442 Regarding DBL-homolog genes, only 5.6% and 44.7% are close to transposase
443 genes on chromosomes and plasmids, respectively. The majority of DBL-homolog
444 genes encoded on chromosomes near a transposase gene (568) are found in
445 *Acinetobacter* (395), which is also the genus in which we identified most DBL-
446 homologs (see section OXA-domain family proteins include BlaR homologs).
447 However, when the genes are plasmid-encoded, those close to a transposase gene
448 (965) are mainly found in *Klebsiella* (345), then *Acinetobacter* (189), *Shigella* (177)
449 and *Escherichia* (112). Furthermore, three DBL-homolog genes in Cyanobacteria
450 (two on a chromosome and one on plasmid) and one chromosome-encoded gene in

Balnealaoeta are close to a transposase gene, which suggests that they might have been acquired by gene transfer. In contigs not classified by PlasFlow, we observed a higher prevalence of DBL-homolog genes than BlaR-homolog genes, and these DBL-homologs are very distant from transposase genes. As this pattern is similar to the pattern observed for chromosomes (Fig. 2b), it indicates that unclassified contigs likely correspond to chromosomes.

Signal peptide and transmembrane segment prediction

Most DBL-homolog sequences are characterized by a signal peptide (SP), as predicted by SignalP (Table 1). The Sec, Lipo and Tat SPs were identified in 65%, 22% and 3% of DBL-homolog unique sequences, respectively (see Enlarging the OXA-domain family distribution). The rest of the sequences (OTHER-SP, 9%) are either transmembrane proteins or have no SP. DBL-homolog sequences with a Sec-SP are mainly found in the genera *Pseudomonas*, *Burkholderia*, *Campylobacter*, *Klebsiella* and *Legionella*, while DBL-homolog sequences with a Lipo-SP were mostly identified in *Acinetobacter* and *Leptospira*. DBL-homologs with a Tat-SP seem to be more specific to Alphaproteobacteria (*Bradyrhizobium*) whereas the "OTHER-SP" prediction is mainly associated with *Clostridioides* CDD enzymes (29).

Beside signal peptide prediction of SignalP, the transmembrane segment (TM) prediction was used to distinguish between membrane proteins and cytoplasmic proteins. Whenever a SP is predicted in DBL-homolog sequences, the TM prediction indicates no TM or, rarely, 1 TM domain (monotopic) (Table 1). When no TM domain is detected, it may indicate that the corresponding DBL-homolog is excreted outside the cell or into the periplasmic space (for diderm bacteria). In contrast, when one TM

20

475 domain is predicted, the protein is more likely to be anchored in the cytoplasmic
476 membrane. In the majority of DBL-homologs with no SP predicted, no TM domain is
477 detected, and these are possibly cytoplasmic proteins. Nevertheless, some
478 exceptions exist, with 60 unique sequences (on 255 unique DBL-homolog proteins
479 with no SP) presenting one or more TM domains (polytopic), a configuration which
480 remains to be explained.
481
482 Almost all the BlaR-homolog proteins have no SP predicted and have, as expected,
483 more than one TM domain (Table 1). However, only three polytopic proteins were
484 predicted with Sec-SP or Lipo-SP instead of OTHER-SP. This can be explained by a
485 wrong attribution by SignalP. Indeed, SignalP gives a probability for each possible
486 SP and then chooses the highest value for the prediction but, for those sequences,
487 the probabilities for OTHER-SP and Sec-SP/Lipo-SP are both close to 0.5.

488 Prevalence of DBL-homolog genes in clinical strains

489 Acquired resistance in clinical bacterial strains is a very important concern, but
490 determining the clinical origin of a given bacterial isolate only based on the metadata
491 of the corresponding genome assembly is still challenging to automate at a large
492 scale. Indeed, BioSample reports from the NCBI can contain such information but
493 these remain difficult to analyze due to the lack of a controlled vocabulary. To
494 overcome this difficulty, we used a script that standardizes all the words of a
495 BioSample report. Thus, 20,317 BioSample accessions were associated with the
496 20,342 bacterial assemblies containing DBL-homolog or BlaR-homolog genes for a
497 total of 223 unique standardized words. Note that 4,658 BioSample reports did not
498 contain any word. BioSamples with a positive clinical score (see Materials and

Methods for details) were considered as clinical strains while those with negative scores were not. Furthermore, we decided to not classify BioSamples with a null score (essentially due the aforementioned lack of words). Using this strategy, 3192 bacteria were classified as *clinical*, 2810 as *non-clinical* and 14,340 could not be classified. Around 28% of the gene sequences belong to classified strains (15.5% belong to clinical strains), of which 34% of the DBL-homolog sequences (Table 2). Clinical DBL-homolog genes encoded on a plasmid are exclusively present in Gammaproteobacteria, mostly in *Acinetobacter* (176), *Klebsiella* (135) and *Enterobacter* (93), while DBL-homolog genes encoded on chromosomes are mostly found in Proteobacteria (2,016) and some in Firmicutes (43), Bacteroidetes (10), Spirochaetes (8), Actinobacteria (2) and Verrucomicrobia (1).

Clustering and DBL-homolog selection

Over 600 combinations of clustering parameters were tested on the OXA-domain family phylogenetic tree (see SQL database) and the clustering with the highest entropy and the lowest number of singletons (i.e. clusters of size one) was retained (x set at 0.20 and inflation at 1.5; see Materials and Methods). This specific clustering solution has a computed entropy of 0.762 and a score of 0.52. It contains 64 clusters, including 19 singletons, with the larger cluster having 207 representative putative sequences (cluster 15) among 1413 (Table S1). In general, there is little taxonomic diversity within each cluster. Indeed, the majority of these clusters (50) contain sequences from organisms belonging to the same phylum or class.

Annotating the unique sequences using BDLB reference sequences at an identity threshold set to 100% (see Materials and Methods) allowed us to tag 340 unique

sequences, corresponding to 307 reference sequences (304 DBL/pseudo-DBL and 3 BlaRs) among 813 BLDB sequences. When decreasing the identity threshold to 99%, 623 unique sequences were tagged with 653 reference sequences (650 DBL/pseudo-DBL and 3 BlaRs), while at 90%, 1269 unique sequences were tagged with 801 reference sequences. All those tagged sequences are distributed across 18 clusters, regardless of the identity threshold. Interestingly, up to half of the reference sequences tag cluster 60 (i.e. 168 sequences at 100%; 363 at 99%; 452 at 90%). The main genus of this cluster composed of 66 representative sequences (standing for a total of 3472 sequences) is *Acinetobacter,* which is the host organism for 99.7% of the sequences. Irrespective of the high-redundancy of cluster 60, the latter genus is known to harbor various chromosome-encoded DBL (10).

Assessment of the beta-lactamase activity in uncharacterized clusters

To test the beta-lactamase activity of some of the 46 non-annotated clusters, ten DBL-homolog sequences were selected for expression and production. Clusters were sorted from the largest to the smallest (considering all and not only representative sequences), then one sequence from the first ten cluster with no DBL found in the BLDB, a sequence length between 250 and 350 AAs and no mutation in the three conserved motifs defining the class D active site. Thus, the ten DBL-homolog (termed OXAVL01 to 10) were selected from clusters 14, 22, 23, 28, 30, 39, 41, 42, 44 and 57 (Table S2). OXAVL01 has the 2 lysines of its active site mutated but these mutations are shared by all the sequences in cluster 14. According to the clinical score (see Prevalence of DBL-homolog genes in clinical strains), none of those DBL-homologs belong to a clinical strain (six classified as non-clinical and four

as unknown). Seven of those sequences are chromosome-encoded while no localisation could be associated to OXAVL05, OXAVL09 and OXAVL10.

The production of OXAVL01-10 was evaluated by SDS-PAGE and beta-lactam hydrolysis. No apparent over-expression of OXAVL01, OXAVL03, OXAVL05, OXAVL07 and OXAVL09 was observed in the soluble or insoluble fractions of *E. coli* (DE3) grown at 18°C and 37°C. For OXAVL04, OXAVL08 and OXAVL10, a large production of the beta-lactamases was found only in the insoluble fractions at both culture temperatures. Only OXAVL02 and OXAVL06 were overproduced as soluble enzymes at 18°C.

The evaluation of the beta-lactamase activity on crude cell extracts (Table 3) showed that only OXAVL02 and OXAVL06 were able to hydrolyze all beta-lactams tested, including imipenem. OXAVL09 was active versus nitrocefin, ampicillin and oxacillin but not imipenem. OXAVL03 was able to hydrolyze nitrocefin and ampicillin. Cell extracts of OXAVL04, OXAVL05 and OXAVL10 were active only against nitrocefin. The DBL-homolog enzymes were not produced in an active form in the strains bearing the plasmid pOXAVL01, pOXAVL07 or pOXAVL08.

OXAVL02 and OXAVL06 have carbapenemase activity

Since crude extracts of OXAVL02 and OXAVL06 were the only ones able to hydrolyze all tested beta-lactams and had the highest level of expression in the soluble fraction, we focused our work on those two hydrolases. The purification of the two enzymes included three chromatographic steps, namely an anion exchanger, an IMAC affinity chromatography and a molecular sieve. For OXAVL02, the purification consists in an IMAC column followed by a strong anion exchanger high

24

resolution SOURCE™ 15Q column. The last step is a size exclusion chromatography (SEC). At the end of the process, we obtained more than 100 mg of pure protein per liter of culture. The three steps of the OXAVL06 purification are a Q sepharose HP ion exchanger, an IMAC column and finally a SEC. For OXAVL06, we obtained 10 mg of pure protein per liter of culture.

SEC experiments revealed that the OXAVL02 elutes in three major peaks (Fig. 3a), with one at an elution volume typical of a monomeric DBL (~260 mL). The two additional peaks elute at about 230 mL and 180 mL, which is similar to the elution volume of the dimer and multimer, respectively. The three peaks displayed an oxacillinase activity. Due to the low precision of oligomeric states of the proteins determined by SEC, we further characterized these three peaks using SEC-MALS (Fig. 3b).

The elution was monitored by a UV detector, a MALS (Multi-Angle Light Scattering) detector, and a differential refractometer in line with the SEC column, allowing for the deconvolution of the protein molar masses (MM) of eluting protein complexes. The major peak in the OXAVL02 sample was confirmed to result from an equilibrium between a major monomeric form with an apparent protein MM of 32,000±1,000 Da [theoretical MM (tMM) 31,298 Da] and a dimer at 62,000±2,000 Da [tMM 62,596 Da]. Of the two other peaks, the lower elution volume peak (at 180 mL) contained large aggregates (apparent MM > $3x10^5$ Da), while the higher elution volume peak (230 mL) corresponded to the approximate MM of a dimer at 62,000±2,000 Da [tMM 62,596 Da] in equilibrium with protein aggregates. Similar data were recorded for OXAVL06 (Fig. S2).

A kinetic profile of the two purified DBL-homologs was performed in the presence of

25

50 mM $NaHCO_3$ (Table 4). Indeed, in absence of hydrogenocarbonate, their activity generally showed an initial burst, followed by a pronounced slowdown, even when the substrate conversion and product accumulation were quite low. Our data indicates that OXAVL02 displays a lower catalytic efficiency compared to OXAVL06. We observed that both enzymes were not able to hydrolyse amoxicillin, temocillin, cefazolin and cefotaxime. In addition, OXAVL06 was not active against piperacillin and meropenem. We confirmed also that the two beta-lactamases displayed a carbapenemase activity. Imipenem was among the best substrates (k_{cat}/K_m = 0.016 and 2.5 $\mu M^{-1}s^{-1}$ for OXAVL02 and OXAVL06, respectively). In comparison to values obtained for oxacillin, the k_{cat}/K_m ratios of OXAVL02 for meropenem and imipenem were 30 and 10-fold higher, respectively.

Discussion

No OXA-domain family protein detected in Archaea

The focus of this study was to explore the occurrence of class D beta-lactamases in the prokaryotic world. The 24,916 identified OXA-domain family sequences correspond to 3510 unique sequences distributed across 20,343 bacterial strains. This highlighted a well-known redundancy in the NCBI RefSeq database toward clinical strains (46) (Fig. S3). The fact that none of these OXA-domain family proteins was detected in Archaea could be expected, since Archaea are naturally resistant to beta-lactam antibiotics. Indeed, even when a pseudomurein is present, the crosslinking of the glycan chains does not involve D-Ala-D-Ala and thus does not hinge on the activity of Penicillin Binding Proteins. However, two recent studies identified class A, B and C beta-lactamase homologues in archaeal genomes and

revealed that archaeal class B and C homologues do show a weak beta-lactamase activity (21, 47). Therefore, although we did not detect OXA-domain family proteins in Archaea, it is possible that archaeal OXA-domain family proteins will be identified in further studies, like for the other classes of beta-lactamases.

Contaminated genomes from local NCBI RefSeq database

Identification of new beta-lactamases in some unexpected organisms like Archaea or non-clinical bacterial strains might seem an exciting finding but could also be artifacts. In 2021 Lupo et al. assessed the contamination level of 111,088 bacterial genomes in the NCBI RefSeq database and found that 1% of the genomes were contaminated at a minimal threshold of 5% (46). For the 20,343 genome assemblies used in the current study, 20,200 results were available, indicating that 143 genomes had been suppressed since then. Among these 20,200 bacterial genomes, 114 showed a contamination level ≥5%. Those 114 genomes are distributed across seven phyla: Proteobacteria (78), Firmicutes (29), Verrucomicrobia (2), Cyanobacteria (2), Chloroflexi (1), Chlorobi (1) and Balneolaeota (1). Obviously, conclusions for contaminated genomes should be taken with caution. For example, the only genome containing a DBL-homolog sequence in the Balneolaeota phylum is contaminated. From our data, it is however difficult to identify if this DBL-homolog is part of the contamination or if it is genuinely part of the genome, possibly acquired from an unknown organism by horizontal gene transfer.

OXA-domain family phylogeny and classification

We inferred the phylogenetic tree using a matrix of the 188 most conserved AAs (around two thirds of typical DBL length) from the 1413 representative OXA-domain

family sequences. Those representative sequences resulted from the deduplication of the 3510 unique sequences at a global identity threshold of 95%, which means that, considering their full length, they are similar to at least 95% of observed identity with member sequences of their deduplication clusters. Then, a phylogenetic clustering of the representative OXA-domain family proteins was computed using the patristic distances taken from the tree (i.e. the sum of the branch lengths between two leaves). This patristic distance quantifies the number of AA substitutions computed by the statistical model of sequence evolution. To select the best clustering parameters, we decided to exclude the clustering solutions with less than 15 clusters. In fact, we noticed that at least half of the OXA-domain family protein sequences regroup into one single large cluster when fewer than 15 clusters are produced. The retained parameters yielded 64 clusters, including 19 of size one (singletons). Despite a larger number of clusters, BLDB reference DBL and pseudo-DBL sequences are distributed in only 16 clusters, while BlaR from *Clostridium difficile* and *Bacillus licheniformis* are found in cluster 15, and BlaR from *Staphylococcus aureus* in cluster 18.

Another objective of this study was to suggest a meaningful classification of OXA-domain family proteins based on their phylogeny. However, the majority of bacterial strains have only one OXA-domain family protein, indicating that these genes are essentially orthologous. Moreover, 50 clusters out of 64 contain sequences from organisms belonging to a single phylum or class, which means that sequence diversity within the OXA-domain family is mostly due to speciation. While it is possible to generate a classification of class D beta-lactamases based on the clustering obtained in this study, our results indicate that a more practical

28

classification should rather include a reference to the species of origin.

Analysis of the BlaR clusters

Because some class D beta-lactamases display more sequence identity with the C-terminal beta-lactam sensing domain of BlaR than with other class D beta-lactamases, it was impossible to avoid retrieving types of proteins in our homology searches. BlaR is also characterized by a N-terminal domain containing four transmembrane helices and a zinc protease module in loop 2 that is activated upon acylation of the C-terminal domain catalytic serine by a beta-lactam antibiotic. This triggers a cascade that eventually leads to the increased expression of either a beta-lactamase or a resistant PBP (19). As a consequence, BlaR has a total length of about 600 AAs. The size was therefore used to discriminate between BlaR-homologs (> 550 AAs) and the DBL-homologs (< 350 AAs). Clusters 16 and 17 exclusively contain BlaR-homologs, while clusters 8, 15 and 18 contain both BlaR- and DBL-homologs (Table S1). Most BlaR-homologs harbor a polar residue as the third residue of the second conserved motif (Table S1) and contain a N-terminal peptidase domain, two specific features of the BlaR receptor. The only exceptions are a few shorter sequences found in cluster 18; which have been removed from the database since we downloaded them, possibly indicating sequencing errors. Two sequences shorter than 550 AAs and labeled as BlaR-homologs are found in cluster 15. They have the typical conserved motifs of BlaR but their N-terminal domain is truncated and likely not functional. In this study we noticed that BlaR-homolog genes are more frequent on a plasmid nearby a transposase gene. A recent study has shown that *Staphylococcus* species have Tn552-like elements carrying the *bla* operon often located on a plasmid (48). The authors hypothesized that the Tn552

29

transposon can mediate the transfer of the *bla* operon from a plasmid to the chromosome. This hypothesis would also fit our results showing a high prevalence of BlaR-homolog genes on plasmids and their proximity with transposase genes.

Analysis of all the 62 DBL-homolog clusters

The size of the DBL-homolog proteins is very homogenous and the only sequences longer than 350 AAs are three fusions between a class D and a class C beta-lactamase (cluster 8), possibly homologous to LRA-13 (20), three sequences with an N-terminal extension (up to 423 AAs in total) in cluster 21, and a fusion with a crotonase domain (1 sequence in cluster 40) of unknown function. The analysis of the active site motifs (Table S1) shows an almost perfect conservation of the three motifs characteristic of the catalytic site (SxxK, SxV and KTG), as well as of the tryptophan in the omega loop, which is important for the stabilization of the carboxylated lysine of the first motif. The most variable position is the second motif valine, which is often substituted by another hydrophobic AA. Some clusters do however diverge from this consensus. Indeed, clusters 13, 29, 35, 36, 45 and 54 contain only one or two sequences and have significantly impaired motifs, which are likely not compatible with a beta-lactamase activity. Cluster 12 (8 representative sequences), which also has poorly conserved motifs, with an absence of catalytic serine in most cases, is very unlikely to display beta-lactamase activity. In contrast, cluster 14 (11 representative sequences) has the following conserved motifs: SxxH, SxH/Q, AS/TG. A sequence from this cluster (OXAVL01) was selected for *in vitro* characterisation. No beta-lactamase activity was measured on a crude extract, but no over-expression was detected in our assays, preventing us from drawing any definitive conclusion. The conserved motifs are however not sufficient to warrant a

30

beta-lactamase activity, as demonstrated by cluster 19 (Table S1), which regroups so far only pseudo-DBL sequences like YbxI or BAC-1 (17, 18).

Probing clusters without class D beta-lactamase representative

Beyond OXAVL01, we have selected nine DBL-homologs among the 45 clusters devoid of reference OXA-domain family proteins to probe their activity. Overall, for seven of the ten sequences selected for evaluation, a beta-lactamase activity was detected at least on crude extracts (Table 3), including two hydrolases active on imipenem (OXAVL02 and OXAVL06). The enzymatic studies of these two DBL-homolog enzymes confirmed that they both display a beta-lactamase activity and hydrolyse efficiently imipenem but that meropenem is only inactivated by OXAVL02. We also showed that the presence of hydrogenocarbonate enhances their catalytic activity, a sign of the necessary carboxylation of the first motif lysine for optimal activity. As already shown for numerous other class D beta-lactamases, the monomeric form OXAVL02 is in equilibrium with the dimeric form, the monomer being the predominant form of the enzyme at the concentration tested. These results, obtained with randomly selected enzymes, confirm that the environmental strains provide a large reservoir of new resistance genes, which include high potential for resistance to carbapenems, a family of last resort antibacterials. The acquisition of such genes by multi-resistant nosocomial strains therefore represent an important threat for the treatment of the related infections. This phenomenon has already been observed with the chromosome-encoded class A CTX-M-3 from *Kluyvera* spp, which is at the origin of the plasmid-borne CTX-M-1-derived cefotaximases produced by clinical isolates (49). This is a reminder of the importance of an adequate use of the available antibiotics to postpone as much as

possible the emergence of new resistance factors.

Predicting activity profiles from amino acid sequences

The most clinically relevant result would be to deduce the activity profile of an enzyme from its AA sequence. However, determining the activity of only one representative DBL-homolog per cluster would not be informative of the specific activity profile of the cluster. In fact, it has been shown that only one mutated AA can alter the activity profile of a DBL (8, 9). Although the sequence similarity between the 1413 representative sequences and their respective member sequences is high (i.e., at least 95% identity), the identity between the sequences within one of the 45 non-singleton phylogenetic cluster is low (i.e., down to 50%) (Table S3). Furthermore, this similarity is certainly undervalued because it is computed from only 188 unambiguously aligned AAs. Altogether, those arguments support that, for now, the activity profile of a DBL-homolog cannot be predicted only based on its AA sequence. This problem is also true for the other classes of beta-lactamases. Solving this would require a major effort for the high throughput biochemical characterization of the enzymes and the determination of their 3D structure, which is more likely correlated with the substrate specificity than the AA sequence. While the first part still represents a significant bottleneck, the recent development in 3D structure prediction with the AlphaFold software (50) has put the second part within reach, and the use of artificial intelligence to predict the activity profile of enzymes is not as far fetched as it used to be.

32

AUTHOR CONTRIBUTIONS

Valérian Lupo performed experiments, analyzed the data, drew the figures, wrote the manuscript and approved the final manuscript. Denis Baurain and Frédéric Kerff conceived the study and designed experiments, analyzed the data, wrote and reviewed the manuscript and approved the final manuscript. Jean-Marie Frère conceived the study, wrote and reviewed the manuscript and approved the final manuscript. Paola Sandra Mercuri performed experiments, wrote the manuscript and approved the final manuscript. Moreno Galleni designed experiments, wrote the manuscript and approved the final manuscript. Bernard Joris analyzed the data, reviewed the manuscript and approved the final manuscript.

ACKNOWLEDGMENTS

VL is supported by a FRIA (Fonds pour la Formation à la Recherche dans l'Industrie et dans l'Agriculture) fellowship of the FRS-FNRS. FK is a research associate of the FRS-FNRS. MG and PSM were supported by the Belgian Federal Public Service Health, Food Chain Safety and Environment [Grant No. RF 17/6317 RU-BLA-ESBL-CPE]. Computational resources were provided through two grants to DB (University of Liège “Crédit de démarrage 2012” SFRD-12/04; FRS-FNRS “Crédit de recherche 2014” CDR J.0080.15). The authors thank Dr Mohammed Terrak and Dr Adrien Boes for useful advice at the initial stage of the project.

REFERENCES

1. Abraham EP, Chain E. 1940. An Enzyme from Bacteria able to Destroy

33

780 Penicillin. Nature 146:837–837.
781 2. Livermore DM. 2000. Antibiotic resistance in staphylococci. Int J Antimicrob
782 Agents 16 Suppl 1:S3-10.
783 3. Davies J, Davies D. 2010. Origins and evolution of antibiotic resistance.
784 Microbiol Mol Biol Rev MMBR 74:417–433.
785 4. Waley SG. 1992. ß-Lactamase: mechanism of action, p. 198–228. *In* Page, MI
786 (ed.), The Chemistry of β-Lactams. Springer Netherlands, Dordrecht.
787 5. Bebrone C, Garau G, Garcia-Saez I, Chantalat L, Carfi A, Dideberg O. 2012. X-
788 ray Structures and Mechanisms of Metallo-ß-Lactamase, p. 41–77. *In* Frère, J-
789 M (ed.), Beta-Lactamases. Nova Science Publishers, New York.
790 6. Bush K. 2018. Past and Present Perspectives on β-Lactamases. Antimicrob
791 Agents Chemother 62.
792 7. Philippon A, Jacquier H, Ruppé E, Labia R. 2019. Structure-based classification
793 of class A beta-lactamases, an update. Curr Res Transl Med 67:115–122.
794 8. Sougakoff W. 2012. Structure of class A beta-lactamases, p. 21–39. *In* Frère, J-
795 M (ed.), Beta-Lactamases. Nova Science Publishers, New York.
796 9. Castanheira M, Simner PJ, Bradford PA. 2021. Extended-spectrum β-
797 lactamases: an update on their characteristics, epidemiology and detection.
798 JAC-Antimicrob Resist 3:dlab092.
799 10. Evans BA, Amyes SGB. 2014. OXA β-lactamases. Clin Microbiol Rev 27:241–
800 263.
801 11. Naas T, Oueslati S, Bonnin RA, Dabos ML, Zavala A, Dortet L, Retailleau P,
802 Iorga BI. 2017. Beta-lactamase database (BLDB) - structure and function. J
803 Enzyme Inhib Med Chem 32:917–919.
804 12. Danel F, Frère JM, Livermore DM. 2001. Evidence of dimerisation among class

D beta-lactamases: kinetics of OXA-14 beta-lactamase. Biochim Biophys Acta 1546:132–142.

13. Golemi D, Maveyraud L, Vakulenko S, Samama JP, Mobashery S. 2001. Critical involvement of a carbamylated lysine in catalytic function of class D beta-lactamases. Proc Natl Acad Sci U S A 98:14280–14285.
14. Ledent P, Frère JM. 1993. Substrate-induced inactivation of the OXA2 beta-lactamase. Biochem J 295 (Pt 3):871–878.
15. Poirel L, Naas T, Nordmann P. 2010. Diversity, epidemiology, and genetics of class D beta-lactamases. Antimicrob Agents Chemother 54:24–38.
16. Zhu YF, Curran IH, Joris B, Ghuysen JM, Lampen JO. 1990. Identification of BlaR, the signal transducer for beta-lactamase production in Bacillus licheniformis, as a penicillin-binding protein with strong homology to the OXA-2 beta-lactamase (class D) of Salmonella typhimurium. J Bacteriol 172:1137–1141.
17. Colombo M-L, Hanique S, Baurin SL, Bauvois C, De Vriendt K, Van Beeumen JJ, Frère J-M, Joris B. 2004. The ybxI gene of Bacillus subtilis 168 encodes a class D beta-lactamase of low activity. Antimicrob Agents Chemother 48:484–490.
18. Toth M, Antunes NT, Stewart NK, Frase H, Bhattacharya M, Smith CA, Vakulenko SB. 2016. Class D β-lactamases do exist in Gram-positive bacteria. Nat Chem Biol 12:9–14.
19. Hardt K, Joris B, Lepage S, Brasseur R, Lampen JO, Frère JM, Fink AL, Ghuysen JM. 1997. The penicillin sensory transducer, BlaR, involved in the inducibility of beta-lactamase synthesis in Bacillus licheniformis is embedded in the plasma membrane via a four-alpha-helix bundle. Mol Microbiol 23:935–944.

20. Allen HK, Moe LA, Rodbumrer J, Gaarder A, Handelsman J. 2009. Functional metagenomics reveals diverse beta-lactamases in a remote Alaskan soil. ISME J 3:243–251.
21. Keshri V, Panda A, Levasseur A, Rolain J-M, Pontarotti P, Raoult D. 2018. Phylogenomic Analysis of β-Lactamase in Archaea and Bacteria Enables the Identification of Putative New Members. Genome Biol Evol 10:1106–1114.
22. Sengupta S, Chattopadhyay MK, Grossart H-P. 2013. The multifaceted roles of antibiotics and antibiotic resistance in nature. Front Microbiol 4:47.
23. Papp-Wallace KM, Endimiani A, Taracila MA, Bonomo RA. 2011. Carbapenems: past, present, and future. Antimicrob Agents Chemother 55:4943–4960.
24. Dewi DAPR, Thomas T, Ahmad Mokhtar AM, Mat Nanyan NS, Zulfigar SB, Salikin NH. 2021. Carbapenem Resistance among Marine Bacteria-An Emerging Threat to the Global Health Sector. Microorganisms 9.
25. Cherak Z, Loucif L, Moussi A, Rolain J-M. 2021. Carbapenemase-producing Gram-negative bacteria in aquatic environments: a review. J Glob Antimicrob Resist 25:287–309.
26. Fu L, Niu B, Zhu Z, Wu S, Li W. 2012. CD-HIT: accelerated for clustering the next-generation sequencing data. Bioinformatics 28:3150–3152.
27. Katoh K, Standley DM. 2013. MAFFT multiple sequence alignment software version 7: improvements in performance and usability. Mol Biol Evol 30:772–780.
28. Eddy SR. 2011. Accelerated profile HMM searches. PLoS Comput Biol 7:e1002195.
29. Toth M, Stewart NK, Smith C, Vakulenko SB. 2018. Intrinsic Class D β-

Lactamases of Clostridium difficile. mBio 9.

30. Almagro Armenteros JJ, Tsirigos KD, Sønderby CK, Petersen TN, Winther O, Brunak S, von Heijne G, Nielsen H. 2019. SignalP 5.0 improves signal peptide predictions using deep neural networks. Nat Biotechnol 37:420–423.
31. Krogh A, Larsson B, von Heijne G, Sonnhammer EL. 2001. Predicting transmembrane protein topology with a hidden Markov model: application to complete genomes. J Mol Biol 305:567–580.
32. Jones P, Binns D, Chang H-Y, Fraser M, Li W, McAnulla C, McWilliam H, Maslen J, Mitchell A, Nuka G, Pesseat S, Quinn AF, Sangrador-Vegas A, Scheremetjew M, Yong S-Y, Lopez R, Hunter S. 2014. InterProScan 5: genome-scale protein function classification. Bioinformatics 30:1236–1240.
33. Rice P, Longden I, Bleasby A. 2000. EMBOSS: the European Molecular Biology Open Software Suite. Trends Genet TIG 16:276–277.
34. Garcia PS, Jauffrit F, Grangeasse C, Brochier-Armanet C. 2019. GeneSpy, a user-friendly and flexible genomic context visualizer. Bioinformatics 35:329–331.
35. Krawczyk PS, Lipinski L, Dziembowski A. 2018. PlasFlow: predicting plasmid sequences in metagenomic data using genome signatures. Nucleic Acids Res 46:e35.
36. Philippe H. 1993. MUST, a computer package of Management Utilities for Sequences and Trees. Nucleic Acids Res 21:5264–5272.
37. Stamatakis A. 2014. RAxML version 8: A tool for phylogenetic analysis and post-analysis of large phylogenies. Bioinformatics 30:1312–1313.
38. Lemoine F, Domelevo Entfellner J-B, Wilkinson E, Correia D, Dávila Felipe M, De Oliveira T, Gascuel O. 2018. Renewing Felsenstein's phylogenetic bootstrap

880 in the era of big data. Nature 556:452–456.
881 39. Hackathon R, Bolker B, Butler M, Cowan P, Vienne D de, Eddelbuettel D,
882 Holder M, Jombart T, Kembel S, Michonneau F, Orme D, O'Meara B, Paradis E,
883 Regetz J, Zwickl D. 2019. phylobase: Base Package for Phylogenetic Structures
884 and Comparative Data. https://CRAN.R-project.org/package=phylobase.
885 40. Jombart T, Balloux F, Dray S. 2010. adephylo: new tools for investigating the
886 phylogenetic signal in biological traits. Bioinforma Oxf Engl 26:1907–1909.
887 41. Jäger ML. 2015. MCL: Markov Cluster Algorithm.
888 https://CRAN.R-project.org/package=MCL.
889 42. Califice S, Baurain D, Hanikenne M, Motte P. 2012. A single ancient origin for
890 prototypical serine/arginine-rich splicing factors. Plant Physiol 158:546–560.
891 43. Steiner D, Forrer P, Stumpp MT, Plückthun A. 2006. Signal sequences directing
892 cotranslational translocation expand the range of proteins amenable to phage
893 display. Nat Biotechnol 24:823–831.
894 44. Wyatt PJ. 2021. Differential light scattering and the measurement of molecules
895 and nanoparticles: A review. Anal Chim Acta X 7–8:100070.
896 45. Cornish-Bowden A. 1995. Fundamentals of Enzyme Kinetics. Portland.
897 https://books.google.be/books?id=_jZzQgAACAAJ.
898 46. Lupo V, Van Vlierberghe M, Vanderschuren H, Kerff F, Baurain D, Cornet L.
899 2021. Contamination in Reference Sequence Databases: Time for Divide-and-
900 Rule Tactics. Front Microbiol 12:755101.
901 47. Diene SM, Pinault L, Armstrong N, Azza S, Keshri V, Khelaifia S, Chabrière E,
902 Caetano-Anolles G, Rolain J-M, Pontarotti P, Raoult D. 2020. Dual RNase and
903 β-lactamase Activity of a Single Enzyme Encoded in Archaea. Life Basel Switz
904 10.

905 48. Sun Z, Zhou D, Zhang X, Li Q, Lin H, Lu W, Liu H, Lu J, Lin X, Li K, Xu T, Bao
906 Q, Zhang H. 2020. Determining the Genetic Characteristics of Resistance and
907 Virulence of the “Epidermidis Cluster Group” Through Pan-Genome Analysis.
908 Front Cell Infect Microbiol 10:274.
909 49. Rodríguez MM, Power P, Radice M, Vay C, Famiglietti A, Galleni M, Ayala JA,
910 Gutkind G. 2004. Chromosome-encoded CTX-M-3 from Kluyvera ascorbata: a
911 possible origin of plasmid-borne CTX-M-1-derived cefotaximases. Antimicrob
912 Agents Chemother 48:4895–4897.
913 50. Jumper J, Evans R, Pritzel A, Green T, Figurnov M, Ronneberger O,
914 Tunyasuvunakool K, Bates R, Žídek A, Potapenko A, Bridgland A, Meyer C,
915 Kohl SAA, Ballard AJ, Cowie A, Romera-Paredes B, Nikolov S, Jain R, Adler J,
916 Back T, Petersen S, Reiman D, Clancy E, Zielinski M, Steinegger M, Pacholska
917 M, Berghammer T, Bodenstein S, Silver D, Vinyals O, Senior AW, Kavukcuoglu
918 K, Kohli P, Hassabis D. 2021. Highly accurate protein structure prediction with
919 AlphaFold. Nature 596:583–589.
920

Table 1. **Distribution of predicted signal peptides in DBL-homolog and BlaR-homolog unique sequences further broken by the number of predicted transmembrane (TM) domains (0: cytoplasmic, 1: monotopic, > 1: polytopic).**

# TM	DBL-homologs				BlaR-homologs			
	Signal Peptide (SP)			No SP	Signal Peptide (SP)			No SP
	Sec	Lipo	Tat	Other	Sec	Lipo	Tat	Other
0	1660	587	83	195	0	0	0	0
1	70	4	2	49	0	0	0	1
> 1	0	0	0	11	2	1	0	845

Table 2. **Distribution of DBL- and BlaR-homolog sequences in clinical, non-clinical and unclassified strains, further broken by type of encoding molecule (chromosome, plasmid or unclassified).**

	Clinical		Non-clinical		Unclassified	
	DBL-homologs	BlaR-homologs	DBL-homologs	BlaR-homologs	DBL-homologs	BlaR-homologs
Chromosome	2,080	459	1,716	696	6,282	4,998
Plasmid	512	515	150	305	1497	2,688
Unclassified	234	67	222	36	871	505

40

Table 3. **Beta-lactamase activity of crude extract (CE) for cells expressing active DBL-homologs. The measurements were performed in 25 mM HEPES buffer (pH 7) at 30°C. NH = No Hydrolysis.**

CE	V_0 (nmol.min^{-1}.mgP^{-1})			
	Nitrocefin	Ampicillin	Oxacillin	Imipenem
OXAVL02	9.5	70	18	4
OXAVL03	1	1	NH	NH
OXAVL04	0.7	NH	NH	NH
OXAVL05	2.	NH	NH	NH
OXAVL06	6	85	100	7
OXAVL09	4	7	4	NH
OXAVL10	0.5	NH	NH	NH

Table 4. **Kinetic parameters of OXAVL02 and OXAVL06 beta-lactamases in 25 mM HEPES pH 7.5+ 50 mM NaCarbonate.** NH = No Hydrolysis. Each kinetic value is the mean of three different measurements; SDs were below 5%.

Antibiotics	OXAVL02			OXAVL06		
	k_{cat} (s^{-1})	Km (μM)	k_{cat}/Km ($\mu M^{-1}s^{-1}$)	k_{cat} (s^{-1})	Km (μM)	k_{cat}/Km ($\mu M^{-1}s^{-1}$)
Ampicillin	20	380	0.055	530	270	2
Carbenicillin	22	400	0.055	380	1400	0.25

41

Piperacillin	3	850	0.0055	NH	NH	NH
Oxacillin	1	690	0.0015	90	160	0.56
Cephaloridine	>12.5	>400	0.030	24	90	0.26
Nitrocefin	Product Inhibition			350	20	17.5
Imipenem	9	550	0.016	0.9	0.4	2.5
Meropenem	0.3	6	0.05	NH	NH	NH

937

42

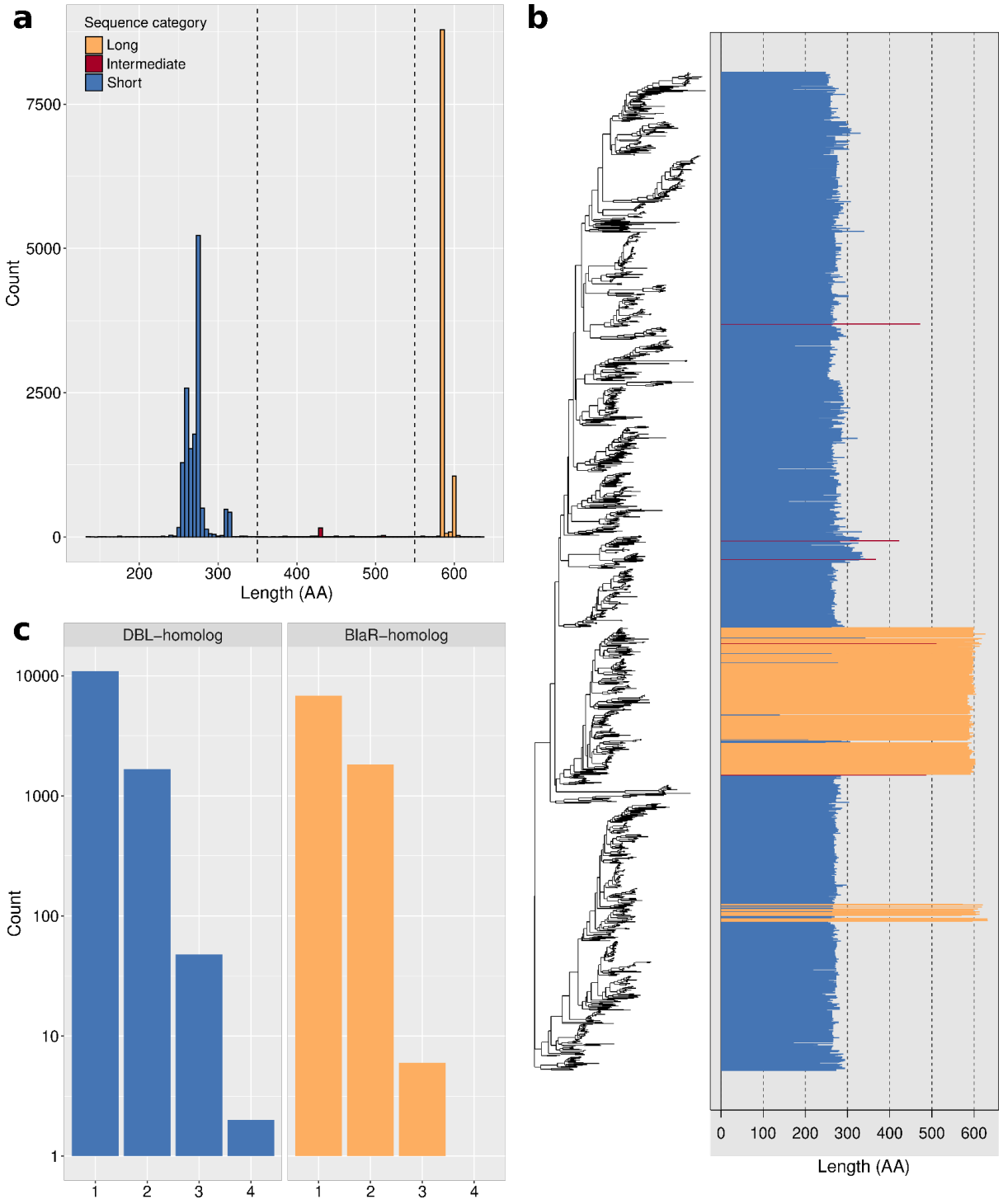

Figure 1. **Classification of OXA-domain family protein sequences as DBL-homologs or BlaR-homologs.** (**a**) Length distribution of the 24,916 OXA-domain family protein sequences. Sequences shorter than 350 AAs are colored in blue, sequences longer than 550 AAs are in orange, while sequences between 350 and 550 AAs are in red. (**b**) Length distribution of the representative sequences mapped

43

944 onto the phylogenetic tree. The tree was constructed from a matrix of 1413
945 representative sequences x 188 unambiguously aligned AAs using RAxML under the
946 LG+F+G4 model. (**c**) Distribution of the number of DBL-homolog and BlaR-homolog
947 sequences per organism. Blue bar plots represent DBL-homolog sequences while
948 orange bar plots represent BlaR-homolog sequences. The Y axis is in log10 units.
949

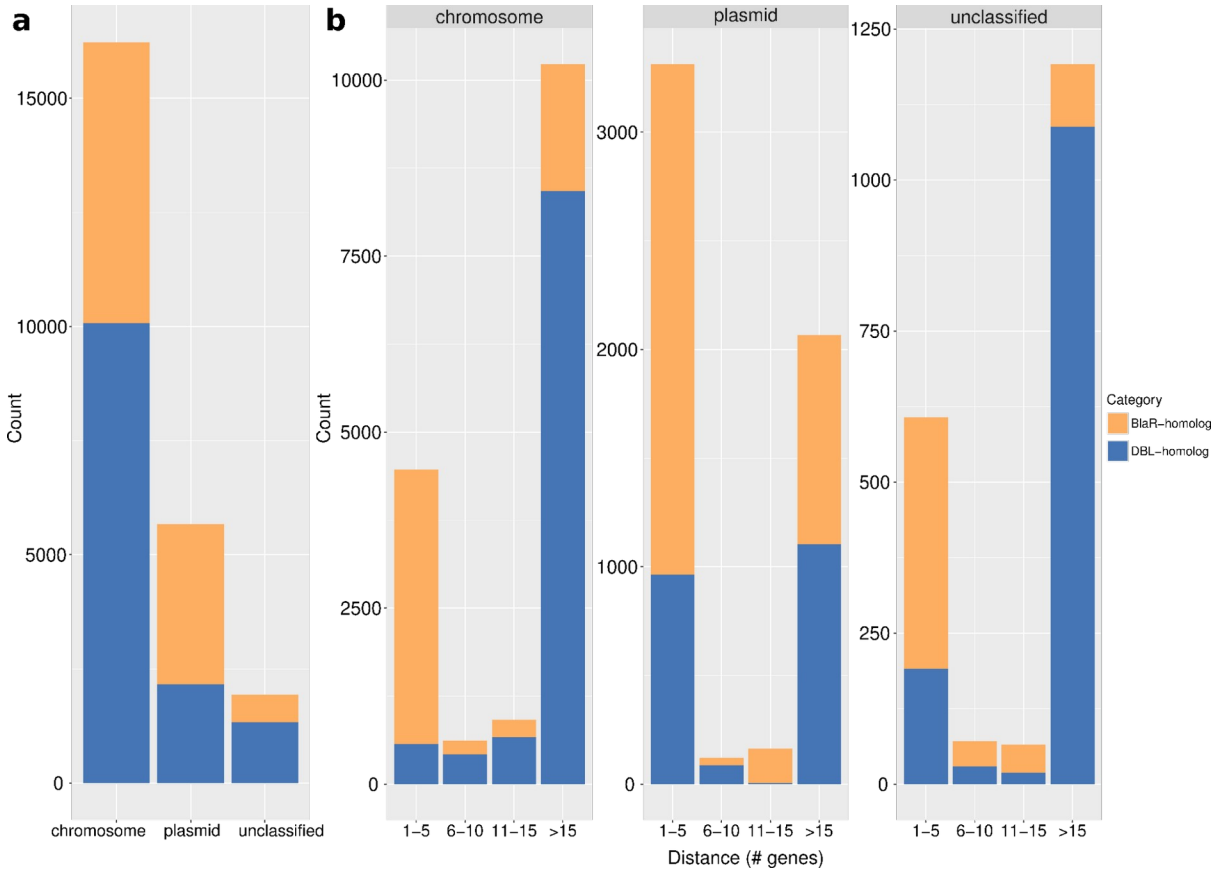

950
951 Figure 2. **DBL-homolog and BlaR-homolog genes in their genetic context.** (**a**)
952 Distribution of DBL- and BlaR-homolog genes according to the type of encoding
953 molecule. (**b**) Distribution of the distances between DBL- and BlaR-homolog genes
954 and transposase genes across the classified contigs. The distance is measured as a
955 range of genes centered on the gene (DBL- or BlaR-homolog) of interest. DBL- and
956 BlaR-homolog genes are colored in blue and orange, respectively.

44

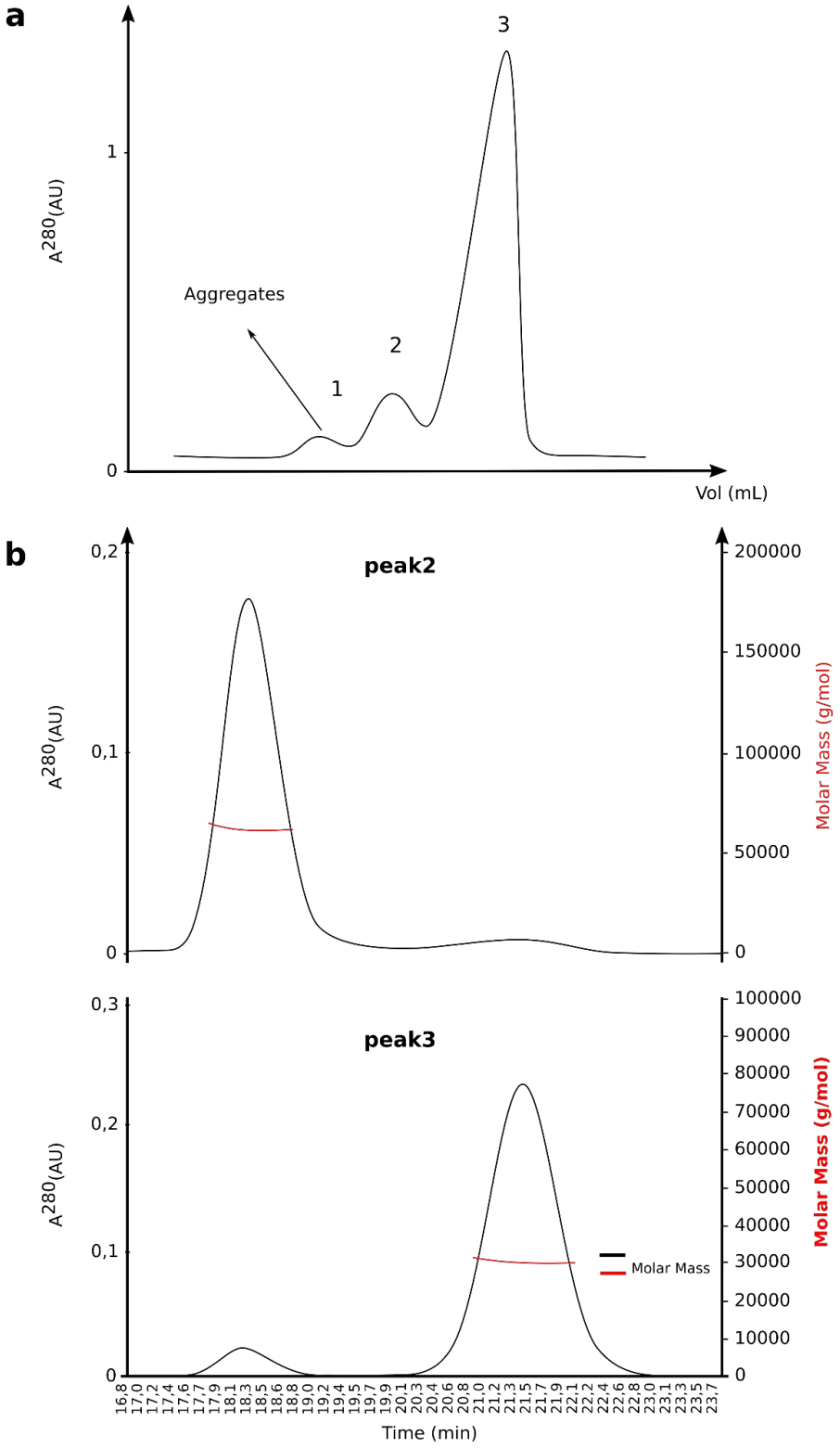

957

958 Figure 3. **SEC and SEC-MALS analysis performed on the purified OXAVL02.** (**a**)

959 SEC analysis of the purified OXAVL02. (**b**) Determination of the multimeric state of

960 OXAVL02 (peaks 2 and 3) by SEC-MALS analysis.